Procedural Image Programs for Representation Learning

Anonymous Author(s)
Affiliation
Address
email

Abstract

Learning image representations using synthetic data allows training neural networks without some of the concerns associated with real images, such as privacy and bias. Existing work focuses on a handful of generative processes which are hard to integrate together to scale up. To overcome this, we propose training with a large dataset of twenty-one thousand programs, each one generating a diverse set of synthetic images. These programs are short code snippets, which are easy to modify and fast to execute using OpenGL. The proposed dataset can be used for both supervised and unsupervised representation learning, and reduces the gap between pre-training with real and procedurally generated images by 38%.

1 Introduction

Training neural networks using data from hand-crafted generative models is a novel approach that allows pre-training without access to real data. This technique has been shown to be effective on downstream tasks for different modalities, such as images [1, 2], videos [3], and text [4]. Despite its big potential, previous work for images is limited, focusing on a handful of generative processes, like fractals [5], textured polygons [3], or dead-leaves and statistical processes [2]. What would happen if we scale this up to *21 thousand* generative image programs?

To this end, we collect a large-scale set of image programs, each producing a diverse set of images that display both shape and texture (see Figures 1 and 2 for examples). We then use these programs to generate images and train neural networks with supervised and unsupervised methods. These networks can then be used on different downstream tasks, reaching state-of-the-art performance for methods that do not pre-train using real images.

The generative programs of this collection are coded in a common language, the OpenGL shading language, that encapsulates the image generation process in a few lines of code. Previous work uses ad-hoc slow methods for each generative process, which makes it hard to integrate them into the same framework. Compared to existing approaches, the rendering of our programs is performed at high throughput (hundreds of frames per second with a single modern GPU), allowing generation on the fly while training.

Furthermore, the dataset consists of a large collection of generative processes allowing training paradigms that were not possible with previous methods. Using each code snippet as a latent class, we can learn representations using supervised approaches. In contrast, previous methods require ad-hoc techniques for clustering the generative parameters into discrete classes [5].

Together with the dataset, the main contributions of the paper are:

Submitted to 36th Conference on Neural Information Processing Systems (NeurIPS 2022). Do not distribute.

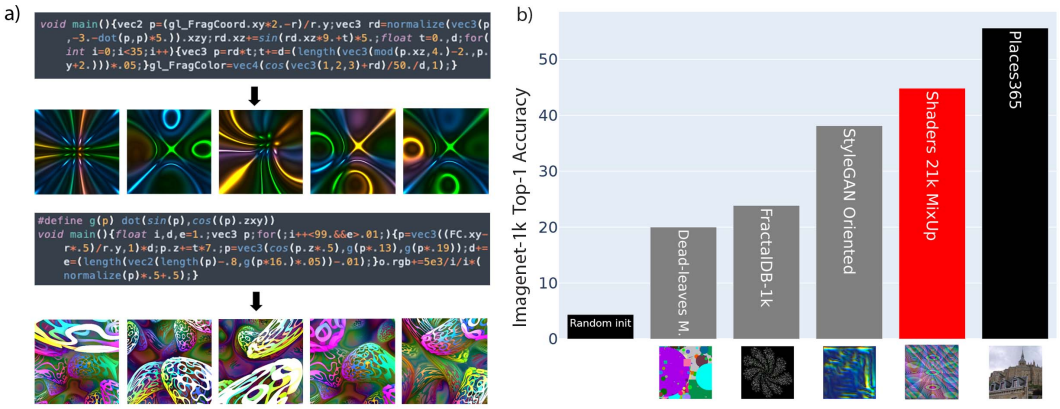

Figure 1: a) We propose learning image representations using a vast collection of short OpenGL fragment shaders (21k). The code and rendered images for two of them are shown. b) Top-1 Accuracy on ImageNet-1k for linear classification with ResNet-50 pre-trained with procedurally generated images from previous methods (Dead-Leaves Mixed [2], FractalDB [1] and StyleGAN Oriented [2], in gray) and our best generative image model, Shaders-21k with MixUp (in red). The lower and upper-bound performance (in black) is for a random initialization and pretraining with Places365 [6].

- A study on how performance scales as a function of the number of generative image programs, for supervised and unsupervised approaches. Our experiments show that downstream performance scales logarithmically with the number of generative programs (see Figure 3 and Section 4).
- State-of-the-art performance for representation learning without real data. When the number of programs is high enough, our approach outperforms equivalent methods by a large margin.
- An analysis of the properties that make for a good image generation program in Section 5. This provides insights on how to design new programs that maximize performance.

To the best of our knowledge, this is the first work to pair a large collection of image generation processes and short programs that is amenable to experimentation. This set of procedural programs has the potential to be a testbed to answer key questions linked to these paired modalities, some of which we answer in this paper. We will release the rendering code and training pipeline upon acceptance.

2 Previous work

Pre-training with synthetic data Pre-training neural networks is a widely used technique to improve performance and convergence speed during training. Typically, pre-trained networks are either used as a starting point in the optimization or to transfer the knowledge from related tasks to the one of interest [7].

When available, pre-training uses real data as close as possible to the task of interest. If the data available for the task is scarce, a common practice is to train on a dataset of natural images, typically ImageNet [8]. These pre-trained models are then used on a wide variety of tasks, achieving state-of-the-art results on tasks with different degrees of similarity to ImageNet. Despite this, it is unclear how much of the performance gain is due to knowledge transfer from the pre-training task or the optimization procedure being simpler to engineer when starting from a pre-trained model [9].

Alternatively, other works achieve state-of-the-art performance by pre-training on synthetic data. These approaches generate realistic-looking images paired with ground-truth annotations, which are then used as pre-training data. Currently, this approach is a standard technique to obtain state-of-the-art performance for low-level vision tasks such as flow estimation [10, 11] and depth prediction [12], between others.

Contrary to these approaches, recent works have studied whether it is necessary to use real-looking data for pre-training. The motivations for doing so are several folds, from targeting domains where

Property		Avg.	Q_5	Q_{95}
# chars	T	283.8	160	662
	S	4307.2	499	$13.6k$
JPEG (KB)	T	70.1	15.0	149.5
	S	53.1	8.8	142.0
gzip (KB/img)	T	57.5	9.8	124.0
	S	42.0	3.6	117.4
FPS	T	886.9	331.0	$1.3k$
	S	984.4	293.5	$1.4k$

Table 1: Dataset properties across shaders for TwiGL (T) and Shadertoy (S), reported as average and 5/95-quantiles over all shaders of each subset. Statistics per shader have been computed with 400 samples at a resolution of 384×384, and rendering time is computed using a single Nvidia GeForce GTX TITAN X, including transfer to general memory.

Figure 2: Example images for a single random timestep t for several random shaders. The first three columns correspond to shaders from TwiGL (Shaders-1k), while the last three columns are shaders from Shadertoy (only included on Shaders-21k). As it is apparent, the complexity, of TwiGL shaders tends to be superior.

rendering would require expert knowledge (like medical imaging), deploying agnostic models to downstream tasks, or making the generative process interpretable and optimizable [3].

In this spirit, the work of [1] introduced a way to train image models using renders with fractal structures. This procedure has been shown to work with different neural architectures [5] and has been further improved with better sampling and colorization strategies [13]. In the same spirit, [2] tested different generative processes to learn general image representations. Their best-performing models are based on neural networks, which are not interpretable and require expert knowledge to manually design.

Representation learning Representation learning is at a level of maturity that shallow networks on top of pre-trained models outperform supervised approaches trained from scratch [14, 15]. Supervised approaches trained on a large corpus with supervision are currently the best representation learners in terms of performance [16]. Despite this, these models inherit the ethical issues associated with the datasets they are trained on. Although they outperform models trained with smaller data collections, this comes at the price of more severe ethical issues, as data curation at a large scale is costly.

On the other hand, unsupervised approaches allow training with unlabeled data, which is usually easier to acquire than labeled data at the same scale by the final users of the models. Once practitioners have pre-trained a model with unlabeled data, they can fine-tune or learn a shallow network on top, which typically requires a substantially smaller amount of annotated data.

The most widely used method for unsupervised representation learning is contrastive learning [17], which has seen consistent improvements in recent years [14, 18]. Contrastive learning is well established and has been shown to perform well in a wide range of image domains, including medical imaging [19] and satellite imagery [20]. Because of this, in this work, we focus on contrastive learning as an unsupervised approach to learning image representations.

Alternatively, early work on unsupervised representation learning focused on pretext tasks that are different from contrastive training, such as context prediction [21] or rotation prediction [22]. Although these initially did not achieve the levels of performance of contrastive approaches, recent work has shown that one of these pretext tasks, masked image prediction with autoencoding, coupled with Vision Transformers [23], can outperform contrastive training in large-scale settings [24]. We do not study these novel approaches as their robustness and broad applicability to different tasks and small training budgets is yet to be studied.

3 The Shaders-1k/21k dataset

The collection of programs we propose consists of a set of generative processes of the form: $g_\theta^i : \mathbf{z} \rightarrow \mathbf{x}$. Each generative program corresponds to the latent class g_θ^i, from which we can produce images x by sampling the stochastic variables z from a prior model. The constant i indexes the programs available, while θ corresponds to the numerical constants of the generative program. In the proposed dataset, each g_θ^i corresponds to an OpenGL fragment shader. Existing similar methods [1, 2] focus on a single type of program ($i = 1$, with variable θ), while this work focuses on a large collection of generative procedures ($i \in \{1, ..., 21k\}$) with fixed θ.

In previous work, the generative programs were designed ad hoc in different programming languages, making it hard to scale or mix different approaches. To overcome this, we fix a common programming language and choose the OpenGL Shading Language, a high-level programming language that allows specifying rendering programs with a syntax based on the C programming language. Furthermore, it is amenable to GPU acceleration, making it particularly suitable to quickly produce images using a standard deep learning stack.

3.1 Program collection

To obtain the desired OpenGL fragment shaders, we query the web for code snippets corresponding to fragment shaders. We obtain them from two sources: Twitter and Shadertoy [25]. The programs obtained from Twitter use the TwiGL syntax as described in [26], which allows extremely compact code (typically less than 280 characters) by abstracting away standard functionalities. On the other hand, Shadertoy is a repository of OpenGL shaders using the standard OpenGL syntax. Shaders in Shadertoy are generally longer (on average 4k characters) and they produce simpler images than those from TwiGL, as the latter are typically coded by more expert users.

The only stochastic variable we consider in practice in the collected shaders is the timestep ($\mathbf{z} = t \in \mathbb{R}$). The parameter t allows generating a continuous video stream, which in lots of cases is periodic. We sample t at 4 frames per second for as many samples as required through all experiments. We add an increment to t sampled at uniform $\Delta t \sim \mathcal{U}[0, 0.25]$, to avoid exact duplicates for the cases where the shader is periodic.

After downloading the code snippets from these two sources, we obtain an initial set of $52k$ shaders that compile with the OpenGL shading language syntax. We first perform duplicate removal by rendering a single image using the same t for all scripts and removing shaders that produce the same images. Additionally, we remove scripts for which different t's produce the same image (i.e. they do not produce videos). With this, we obtain a final set of 1.089 fragment shaders from TwiGL and 19.994 from Shadertoy, which are unique and generate a diverse set of images when varying t.

In Table 1, we report the main characteristics of the shaders and the images they produce. Combining all the shaders from both sources, images can be rendered at 979 frames per second at a resolution of 384×384, using a single modern GPU and including transfer to general memory. When stored to disk as JPEG, the average size per image is 54 kB, compared to 70 kB for ImageNet-1k when resized to the same resolution.

Shaders-1k/21k From a qualitative analysis and the compression results of the generated images in Table 1, we further conclude that TwiGL shaders are more curated and of higher quality than those obtained from Shadertoy (see Figure 2 for examples of both). To distinguish and experiment with both sources, we refer to the dataset composed of only TwiGL shaders as Shaders-1k and the dataset consisting of all available shaders from both sources as Shaders-21k.

4 Experiments

4.1 Supervised vs Unsupervised representation learning

To test downstream performance when pre-training with Shaders-1k and Shaders-21k, we perform an initial set of experiments with and without latent class supervision. We test three representation learning methodologies: supervised classification with cross-entropy loss (CE), supervised contrastive learning (SupCon) [27], and unsupervised representation learning (SimCLR) [14].

Dataset	S.CLR	CE	S.Con
Random init.	17.10	17.10	17.10
Places	<u>52.20</u>	50.7	<u>55.22</u>
I-100	60.30	78.2	80.18
S.GAN O.	44.60	-	-
D.leaves M.	30.56	-	-
FracDB-1k	33.12	26.5	32.98
S-1k	43.26	41.2	40.54
S-21k	47.74	40.3	**48.10**

Table 2: Top-1 accuracy with linear evaluation on ImageNet-100, for a ResNet-18 pre-trained with supervised methods (CE and SupCon) and an unsupervised method (SimCLR), with 100k examples and all the classes (if available). <u>Underlined</u> results are upper bounds for real images.

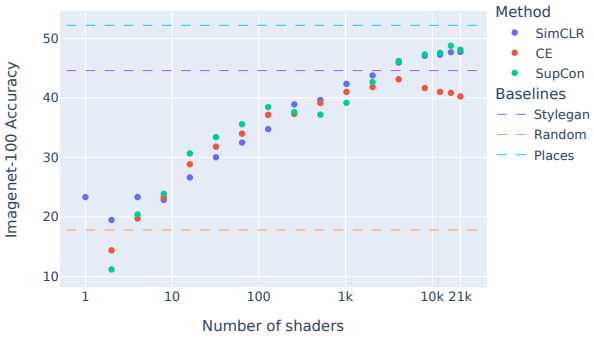

Figure 3: Linear classification performance on ImageNet-100 using a ResNet-18 trained with three representation learning methods and 100k images while varying the number of shaders. As dashed lines, we show performance with SimCLR trained on StyleGAN Oriented (state-of-the-art baseline), Places365 (upper bound), and a random network (lower bound).

To compare these training methodologies, we train a ResNet-18 with 100k samples generated for each dataset at a resolution of 256×256. We follow the training procedure and public implementation described in [27] for the three methods. We train for 200 epochs with a batch size of 256, with the rest of the hyperparameters set to those found to work well for ImageNet-100 in the original paper. The images after augmentations are fed to the network at a resolution of 64×64. After training the encoder, we evaluate using the linear protocol described in [17], which consists of only training a linear classifier on top of the representations learned. We evaluate on ImageNet-100, a subset of ImageNet-1k [8] defined in [28] using the averaged pooled features from the last convolutional layer, which have a dimensionality of 512.

As shown in Table 2, we compare performance using the shader datasets against Places365 [6], which was proposed in [2] as an upper bound for real images when testing on ImageNet; two procedurally generated datasets, FractalDB [1] and Dead Leaves with mixed shapes [2]; and the state of the art for training without real data, StyleGAN Oriented [2].

Shaders-21k using SupCon achieves the best performance over existing methods that do not use real data, but it is closely followed by the same dataset when using SimCLR. Both methods performing equally is expected in this case, as the number of class positives per batch decreases with the number of classes in the dataset. In this experiment, the batch size is relatively small (256) compared to the number of classes (21k). As the number of classes increases, the SupCon loss tends to be equivalent to SimCLR loss, and in the limit of having as many classes as training samples, they are the same.

Using this setting, we test performance for an increasing number of generative programs, sampled at random from Shaders-21k. In this experiment, the number of images is kept constant at 100k while the number of shaders increases (i.e. with more shaders, there are fewer images per shader). As seen in Figure 3, we observe that supervision is helpful in the middle regime where there are more than 20 shaders but less than 1000 shaders, but fails to outperform unsupervised approaches outside this regime. We also note from this sweep that performance is not saturated at 21k shaders, although it scales logarithmically with the number of shaders.

Finally, we also note from this sweep that using the full set of Shaders-1k outperforms a random subset of Shaders-21k of the same size. Shaders-1k achieves higher top-1 accuracy on ImageNet-100 (43.26) compared to a random subset of 1089 shaders obtained from Shaders-21k (42.26). This further verifies that the shaders of Shaders-1k are on average of higher quality than those on Shaders-21k, as hypothesized in Section 3.

Pre-train Dataset	I-1k	I-100	VTAB Nat.	VTAB Spec.	VTAB Struct.
Random init	4.36	10.84	10.98	54.30	22.64
Places365 [6]	<u>55.59</u>	<u>76.00</u>	<u>59.72</u>	84.19	33.58
ImageNet-1k	67.50	86.12	65.90	<u>85.02</u>	<u>35.59</u>
StyleGAN O. [2]	<u>38.12</u>	<u>58.70</u>	<u>54.19</u>	<u>81.70</u>	<u>**35.03**</u>
StyleGAN O. [2] (MixUp)	31.73	53.44	51.26	81.39	33.21
FractalDB-1k [1]	23.86	44.06	38.80	76.93	31.01
Dead-leaves Mixed [2]	20.00	38.34	35.87	74.22	30.81
S-1k	16.67	34.56	32.39	75.28	28.23
S-1k MixUp	38.42	60.04	53.24	82.08	30.32
S-21k	30.25	51.52	45.23	80.75	32.85
S-21k MixUp	**44.83**	**66.36**	**57.18**	**84.08**	31.84

Table 3: Top-1 accuracy with linear evaluation on ImageNet-1k/100 and the VTAB suite of datasets (averaged over the Natural, Specialized, and Structured categories), for a ResNet-50 trained with MoCo V2 with 1.3M samples for each of the pre-training datasets. <u>Underlined</u> results correspond to an upper bound (training with natural images different than the evaluation distribution) and the previous state-of-the-art without real data StyleGAN Oriented [2].

4.2 Large scale unsupervised training

Following the observation that contrastive training performs better than classification to pre-train feature extractors, we extend the previous approach to a large-scale setting. In this setting, we train a ResNet-50 using MoCo v2 [18], with images generated at 384×384 resolution. We train for 200 epochs with 1.3M images, with a batch size of 256, and set the rest of the hyperparameters to those found to work best on ImageNet-1k in the original paper. In Table 3, we show downstream performance for ImageNet-1k and ImageNet-100 and the 19 datasets of the Visual Task Adaptation Benchmark [29], averaged over the natural, specialized and structured categories.

When using data directly rendered from Shaders-1/21k, the performance is low compared to existing methods. We observe that the contrastive loss is lower for Shaders-1k compared to ImageNet-1k (6.2 and 6.6), while top-1 accuracy for the contrastive task is much worse for Shaders-1k (12.5% and 92.2% respectively). This points out that the network is able to solve the contrastive task properly on average (i.e. it is highly confident on most of the 64k negatives in the MoCo buffer), while it is highly confused by a few of the negative samples, which correspond to images from the same shader.

We hypothesize that this is caused by a large capacity network being able to learn shortcut solutions for the contrastive task [30], which results in learned features that do not transfer to downstream tasks. As can be seen from examples in Figure 2, it is easy for a large capacity network to distinguish different shaders via shortcut solutions, like background color or salient features, even after MoCo v2 image augmentations.

To overcome this, we propose mixing samples from different shaders in order to produce interpolated samples in pixel space. This removes some of the shortcut solutions while preserving the complexity of the underlying processes being mixed. We investigate three well-known mixing strategies: CutMix [31], MixUp [32], and producing samples from a GAN [33] that has been trained on the shaders. MixUp has been previously studied in the context of unsupervised contrastive learning [34], showing improved performance in the case where the train time distribution is aligned with the test time distribution.

Using FID computed with 50k samples with respect to ImageNet-100, we conclude that MixUp outperforms the other two strategies (details in Supp. Mat.). This metric was found to correlate with downstream performance in [2], and allows searching for good hyperparameters without training. For the MixUp strategy, we found that mixing 6 frames with weights sampled from a Dirichlet distribution with $\alpha_i = 1$ yields the best FID, while rendering time is still affordable.To be fair against previous methods, MixUp is performed offline before training starts, so that the diversity at training time is the same for all datasets (i.e. 1.3M fixed images, with the same MoCo v2 augmentations across all experiments).

Figure 4: 5 nearest neighbors on ImageNet-100 for ResNet-50 randomly initialized (left) or trained with MoCo v2 on Shaders-21k with MixUp (middle) and Places (right). Reported accuracy correspond to 5-NN accuracy on ImageNet-100.

As seen in Table 3, training with MixUp greatly outperforms the raw shaders. Shaders-21k with MixUp achieves the best performance overall on ImageNet-1k/100 and outperforms the previous state-of-the-art by a substantial margin: an extra 6.71% top-1 accuracy on ImageNet-1k. This represents a 38% relative improvement for the gap between real images different than ImageNet-1k (Places365), and the previous state-of-the-art for procedural images, StyleGAN Oriented. In Figure 4 we show 5 nearest-neighbors retrieval on Imagenet-100 for our best model against a random initialized network and places (additional results for other networks can be found in Supp.Mat.). As can be seen, nearest neighbors successfully retrieve good candidates given a query, capturing different perceptual aspects of the image that are not captured with a randomly initialized model.

We note that StyleGAN Oriented [2] does not improve with the MixUp strategy, achieving worse downstream performance than with the original samples. This is consistent with the FID metric, as the samples with MixUP yield worse (higher) FID than the samples without (38.74 vs 37.74).

In the case of VTAB, Shaders-1k/21k with MixUp outperforms the baselines for natural and specialized tasks, in the case of specialized tasks being close to Places performance. On the other hand, Shaders-1k/21k without mixing outperform their MixUp alternative on structured tasks, although performance for structured tasks is generally low for methods trained with contrastive learning. This is because structured tasks require information about counts, position, or size of the elements in the images, and this information is lost given the invariances that the data augmentations impose [35]. From the results per dataset (see Supp. Mat.), it can be seen that Shaders-1k performs well (even better than ImageNet) on datasets that resemble shaders, as is the case for dSprites dataset, which consists of 2D shapes procedurally generated.

Finally, we use the fact that the Shaders dataset allows rendering novel samples during train time to train with the same procedure, but with a live generator (i.e. the samples for each of the 200 epochs are different). This methodology requires twice as much time to train with the same setup, as the GPU is shared by the rendering and the training, while only improving performance by a small margin, achieving a top-1 accuracy on ImageNet-1k/100 of 45.24% and 66.42%, respectively. This shows that scaling up the number of samples per shader has limited benefits, as this corresponds to 200 times more samples (corresponding to the 200 epochs) than the results presented in Table 3.

5 What makes for a good generative image program?

A single shader: To test what properties of a single shader are useful for downstream performance, we train a ResNet-18 with SimCLR as described in Section 4.1 for each shader in Shaders-1k. We use 10k images from each of the programs in Shaders-1k, train the ResNet-18 for 100 epochs, and then compute performance with linear evaluation for 100 epochs on a random subset of 10k images from ImageNet-100. As shown in Figure 5, there is substantial variability in performance between each of the shaders, and one of the main qualitative drivers is the diversity between samples.

With the performance computed for each of the shaders in Shaders-1k, we train two shallow networks, consisting of two linear layers with ReLu and a hidden dimension of 32 to predict performance per shader. The inputs to the shallow network are the features extracted with the ResNet-50 trained with MoCo v2 for Shaders-1k with MixUp in Section 4.2. We train using an L1-loss to regress

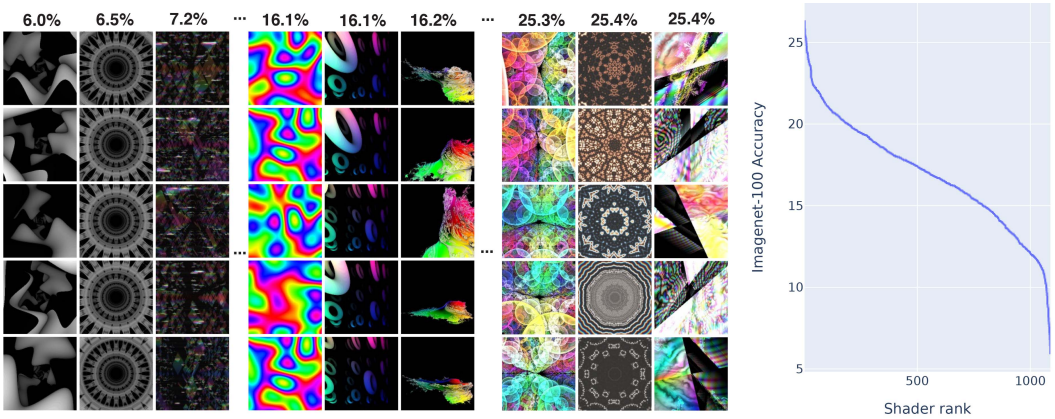

Figure 5: **Left:** Performance for the shaders in Shaders-1k trained with SimCLR on 10k images, evaluated on 10k samples of ImageNet-100. Left-to-right: images for different shaders sorted by performance (on top of each block). **Right:** I-100 accuracy of shaders in Shaders-1k, sorted by rank.

Figure 6: I-100 Performance against FID, LPIPS self-similarity, rendering time (frames per second), and gzip compression (for 400 images). Performance increases with lower FID (activations more similar to ImageNet images), lower self-similarity, higher rendering-time (low FPS), and higher gzip file size, though the correlation is weak except for LPIPS self-similarity.

top-1 accuracy for each shader, splitting them 85-15 into train-val. Of the two trained networks, one gets information from 50 frames (the concatenated average, minimum, and maximum of the activations) while the other only takes a single image as input. We use these networks for the rest of the experiments in this section, depending on whether the phenomena studied requires predicting performance from a single or multiple frames.

With the network that gets information from 50 frames, we rank all the shaders in Shaders-21k. In Figure 7 we show the shader with the best-predicted performance over all Shaders-21k, which: 1) qualitatively is more diverse than the top-performing in Shaders-1k (seen in Figure 5 2) its top-1 accuracy with the comparable training setup is 36%, considerably higher than the 26% achieved for the best shader Shaders-1k.

Additionally, in Figure 6 we show scatter plots for several simple properties of the generated images for each shader against their performance. As can be seen, the metric that best correlates with performance ($r = 0.46$) is LPIPS intra-image distance, matching the findings in [2]. LPIPS [36] is a perceptual similarity metric that has been found to align better with human judgment than other alternatives. LPIPS intra-image is defined as the average LPIPS distance for two random crops covering 50% of a given image, and was first proposed in [37]. Consequently, we conclude that shaders that produce images with high self-similarity tend to perform poorly.

On the other hand, although FID and gzip compression have a low correlation with performance, the plots show that there is a Pareto frontier for both metrics, where shaders cannot achieve high accuracy with low compression or high FID. Performance as a function of rendering time also suggest that there is a big margin to improve it, as the correlation between rendering time and performance is weak and there are lots of shaders that perform well while their rendering time is low.

A collection of shaders: In the same spirit, we consider what makes a collection of shaders perform well or bad when treated as a set, and whether it is possible to achieve increasingly better performance

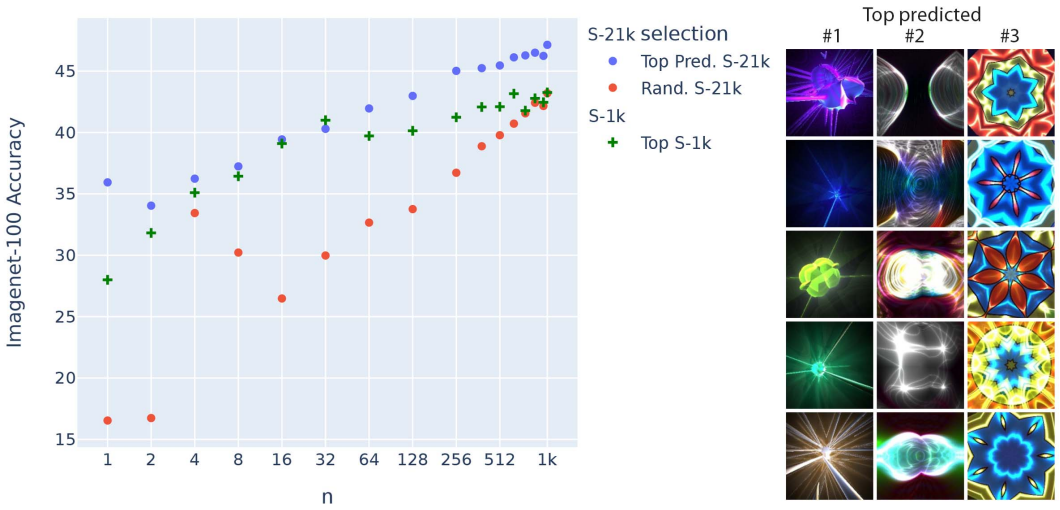

Figure 7: I-100 Top-1 accuracy with 100k images and SimCLR with different sets of shaders selected: 1) at random from Shaders-21k and 2) by predicted performance from all Shaders-21k that remain unseen while training the predictor. As a reference, we also plot performance for the top shaders of Shaders-1k, but we note that this is a more limited set than the full Shaders-21k. The right-most columns are images from the top predicted shaders from Shaders-21k , the best best-performing one achieving 36% top-1 accuracy empirically, compared to 26% for the best in Shaders-1k.

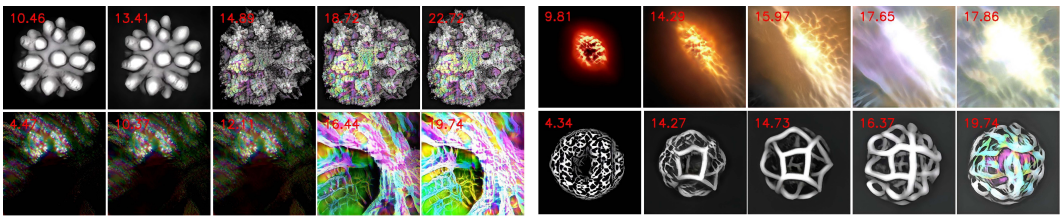

Figure 8: Walks on z space for a StyleGAN trained with Shaders-1k, starting at a random z (center column of each block) and following the trajectory that minimizes (first two columns) or maximizes (last two columns) performance. Factors that drive the performance include color diversity, filling the whole canvas, and intra-diversity, following the findings of the metrics in Figure 6.

with a fixed number of shader programs. With the trained performance predictor per shader as in Section 5, we compute the expected performance for all shaders in Shaders-21k that are not part of Shaders-1k. In Figure 7 we compare using a variable number of shaders selected either by predicted performance or at random. As seen in the figure, the greedy approach of selecting the best-predicted performing shader each time outperforms by a big margin random selection.

Finally, as a qualitative experiment of the properties of the Shaders-1k dataset that make for a good shader, we explore the space of a StyleGAN v2 trained with Shaders-1k. We use the shallow predictor that only takes features from a single image to do so. Then, we explore StyleGAN space by tracing walks in the embedding space z, in the directions that minimize or maximize performance. As Figure 8 shows, samples that improve performance are more colorful and fill the canvas. On the other hand, samples obtained after traversing z in the direction that minimizes performance tend to collapse to repetitive shapes, gray-scale images, or big regions of the image being of a solid color.

6 Conclusions

In this paper, we have proposed using a large collection of procedural image programs to learn data-free representations. As experiments show, training with shaders outperforms existing methods that do not use real data. Using these procedural image models is competitive against natural images, especially in domains far away from the natural image domain, as demonstrated in the specialized tasks in VTAB.

References

[1] Hirokatsu Kataoka, Kazushige Okayasu, Asato Matsumoto, Eisuke Yamagata, Ryosuke Yamada, Nakamasa Inoue, Akio Nakamura, and Yutaka Satoh. Pre-training without natural images. *CoRR*, abs/2101.08515, 2021.

[2] Manel Baradad, Jonas Wulff, Tongzhou Wang, Phillip Isola, and Antonio Torralba. Learning to see by looking at noise. In *Advances in Neural Information Processing Systems*, 2021.

[3] Deqing Sun, Daniel Vlasic, Charles Herrmann, Varun Jampani, Michael Krainin, Huiwen Chang, Ramin Zabih, William T Freeman, and Ce Liu. Autoflow: Learning a better training set for optical flow. In *CVPR*, 2021.

[4] Kundan Krishna, Jeffrey P. Bigham, and Zachary C. Lipton. Does pretraining for summarization require knowledge transfer? *CoRR*, abs/2109.04953, 2021.

[5] Kodai Nakashima, Hirokatsu Kataoka, Asato Matsumoto, Kenji Iwata, and Nakamasa Inoue. Can vision transformers learn without natural images? In *CoRR:2103.13023*, 2021.

[6] Bolei Zhou, Agata Lapedriza, Aditya Khosla, Aude Oliva, and Antonio Torralba. Places: A 10 million image database for scene recognition. *IEEE Transactions on Pattern Analysis and Machine Intelligence*, 2017.

[7] Fuzhen Zhuang, Zhiyuan Qi, Keyu Duan, Dongbo Xi, Yongchun Zhu, Hengshu Zhu, Hui Xiong, and Qing He. A comprehensive survey on transfer learning. *CoRR*, abs/1911.02685, 2019.

[8] Jia Deng, Wei Dong, Richard Socher, Li-Jia Li, Kai Li, and Li Fei-Fei. Imagenet: A large-scale hierarchical image database. In *2009 IEEE conference on computer vision and pattern recognition*, pages 248–255. Ieee, 2009.

[9] Kaiming He, Ross B. Girshick, and Piotr Dollár. Rethinking imagenet pre-training. *2019 IEEE/CVF International Conference on Computer Vision (ICCV)*, pages 4917–4926, 2019.

[10] A. Dosovitskiy, P. Fischer, E. Ilg, P. Häusser, C. Hazırbaş, V. Golkov, P. v.d. Smagt, D. Cremers, and T. Brox. Flownet: Learning optical flow with convolutional networks. In *IEEE International Conference on Computer Vision (ICCV)*, 2015.

[11] Zachary Teed and Jia Deng. RAFT: recurrent all-pairs field transforms for optical flow. In *Computer Vision - ECCV 2020 - 16th European Conference, Glasgow, UK, August 23-28, 2020, Proceedings, Part II*, volume 12347 of *Lecture Notes in Computer Science*, pages 402–419. Springer, 2020.

[12] Cho-Ying Wu, Jialiang Wang, Michael Hall, Ulrich Neumann, and Shuochen Su. Toward practical self-supervised monocular indoor depth estimation. *CoRR*, abs/2112.02306, 2021.

[13] Connor Anderson and Ryan Farrell. Improving fractal pre-training. In *WACV*, pages 1300–1309, 2022.

[14] Ting Chen, Simon Kornblith, Mohammad Norouzi, and Geoffrey Hinton. A simple framework for contrastive learning of visual representations. In Hal Daumé III and Aarti Singh, editors, *Proceedings of the 37th International Conference on Machine Learning*, volume 119 of *Proceedings of Machine Learning Research*, pages 1597–1607. PMLR, 13–18 Jul 2020.

[15] Alec Radford, Jong Wook Kim, Chris Hallacy, Aditya Ramesh, Gabriel Goh, Sandhini Agarwal, Girish Sastry, Amanda Askell, Pamela Mishkin, Jack Clark, Gretchen Krueger, and Ilya Sutskever. Learning transferable visual models from natural language supervision. *CoRR*, abs/2103.00020, 2021.

[16] Alexander Kolesnikov, Lucas Beyer, Xiaohua Zhai, Joan Puigcerver, Jessica Yung, Sylvain Gelly, and Neil Houlsby. Big transfer (bit): General visual representation learning. *arXiv preprint arXiv:1912.11370*, 6(2):8, 2019.

[17] Aäron van den Oord, Yazhe Li, and Oriol Vinyals. Representation learning with contrastive predictive coding. *CoRR*, abs/1807.03748, 2018.

[18] Xinlei Chen, Haoqi Fan, Ross B. Girshick, and Kaiming He. Improved baselines with momentum contrastive learning. *CoRR*, abs/2003.04297, 2020.

[19] Krishna Chaitanya, Ertunc Erdil, Neerav Karani, and Ender Konukoglu. Contrastive learning of global and local features for medical image segmentation with limited annotations. *Advances in Neural Information Processing Systems*, 33, 2020.

[20] Oscar Mañas, Alexandre Lacoste, Xavier Giró-i Nieto, David Vazquez, and Pau Rodríguez. Seasonal contrast: Unsupervised pre-training from uncurated remote sensing data. In *Proceedings of the IEEE/CVF International Conference on Computer Vision (ICCV)*, pages 9414–9423, October 2021.

[21] Carl Doersch, Abhinav Gupta, and Alexei A. Efros. Unsupervised visual representation learning by context prediction. In *International Conference on Computer Vision (ICCV)*, 2015.

[22] Spyros Gidaris, Praveer Singh, and Nikos Komodakis. Unsupervised representation learning by predicting image rotations. In *International Conference on Learning Representations*, 2018.

[23] Alexey Dosovitskiy, Lucas Beyer, Alexander Kolesnikov, Dirk Weissenborn, Xiaohua Zhai, Thomas Unterthiner, Mostafa Dehghani, Matthias Minderer, Georg Heigold, Sylvain Gelly, Jakob Uszkoreit, and Neil Houlsby. An image is worth 16x16 words: Transformers for image recognition at scale. In *International Conference on Learning Representations*, 2021.

[24] Kaiming He, Xinlei Chen, Saining Xie, Yanghao Li, Piotr Dollár, and Ross B. Girshick. Masked autoencoders are scalable vision learners. *CoRR*, abs/2111.06377, 2021.

[25] Shadertoy. Shadertoy. `https://www.shadertoy.com/`, 2021. Accessed: 2022-05-15.

[26] TwiGL. Twigl. `https://github.com/doxas/twigl`, 2021. Accessed: 2022-05-15.

[27] Prannay Khosla, Piotr Teterwak, Chen Wang, Aaron Sarna, Yonglong Tian, Phillip Isola, Aaron Maschinot, Ce Liu, and Dilip Krishnan. Supervised contrastive learning. In H. Larochelle, M. Ranzato, R. Hadsell, M. F. Balcan, and H. Lin, editors, *Advances in Neural Information Processing Systems*, volume 33, pages 18661–18673. Curran Associates, Inc., 2020.

[28] Yonglong Tian, Dilip Krishnan, and Phillip Isola. Contrastive multiview coding. *CoRR*, abs/1906.05849, 2019.

[29] Xiaohua Zhai, Joan Puigcerver, Alexander Kolesnikov, Pierre Ruyssen, Carlos Riquelme, Mario Lucic, Josip Djolonga, André Susano Pinto, Maxim Neumann, Alexey Dosovitskiy, Lucas Beyer, Olivier Bachem, Michael Tschannen, Marcin Michalski, Olivier Bousquet, Sylvain Gelly, and Neil Houlsby. The visual task adaptation benchmark. *CoRR*, abs/1910.04867, 2019.

[30] Joshua Robinson, Li Sun, Ke Yu, Kayhan Batmanghelich, Stefanie Jegelka, and Suvrit Sra. Can contrastive learning avoid shortcut solutions? *NeurIPS*, 2021.

[31] Sangdoo Yun, Dongyoon Han, Seong Joon Oh, Sanghyuk Chun, Junsuk Choe, and Youngjoon Yoo. Cutmix: Regularization strategy to train strong classifiers with localizable features. In *International Conference on Computer Vision (ICCV)*, 2019.

[32] Hongyi Zhang, Moustapha Cisse, Yann N. Dauphin, and David Lopez-Paz. mixup: Beyond empirical risk minimization. In *International Conference on Learning Representations*, 2018.

[33] Ali Jahanian, Xavier Puig, Yonglong Tian, and Phillip Isola. Generative models as a data source for multiview representation learning. *arXiv preprint arXiv:2106.05258*, 2021.

[34] Zhiqiang Shen, Zechun Liu, Zhuang Liu, Marios Savvides, and Trevor Darrell. Rethinking image mixture for unsupervised visual representation learning. *CoRR*, abs/2003.05438, 2020.

[35] Tete Xiao, Xiaolong Wang, Alexei A Efros, and Trevor Darrell. What should not be contrastive in contrastive learning. In *International Conference on Learning Representations*, 2021.

[36] Richard Zhang, Phillip Isola, Alexei A Efros, Eli Shechtman, and Oliver Wang. The unreasonable effectiveness of deep features as a perceptual metric. In *CVPR*, 2018.

[37] Jun-Yan Zhu, Richard Zhang, Deepak Pathak, Trevor Darrell, Alexei A Efros, Oliver Wang, and Eli Shechtman. Toward multimodal image-to-image translation. In I. Guyon, U. V. Luxburg, S. Bengio, H. Wallach, R. Fergus, S. Vishwanathan, and R. Garnett, editors, *Advances in Neural Information Processing Systems 30*, pages 465–476. Curran Associates, Inc., 2017.

Checklist

The checklist follows the references. Please read the checklist guidelines carefully for information on how to answer these questions. For each question, change the default **[TODO]** to [Yes] , [No] , or [N/A] . You are strongly encouraged to include a **justification to your answer**, either by referencing the appropriate section of your paper or providing a brief inline description. For example:

- Did you include the license to the code and datasets? [Yes] See Section **??**.
- Did you include the license to the code and datasets? [No] The code and the data are proprietary.
- Did you include the license to the code and datasets? [N/A]

Please do not modify the questions and only use the provided macros for your answers. Note that the Checklist section does not count towards the page limit. In your paper, please delete this instructions block and only keep the Checklist section heading above along with the questions/answers below.

1. For all authors...
   (a) Do the main claims made in the abstract and introduction accurately reflect the paper's contributions and scope? [Yes]
   (b) Did you describe the limitations of your work? [Yes]
   (c) Did you discuss any potential negative societal impacts of your work? [Yes]
   (d) Have you read the ethics review guidelines and ensured that your paper conforms to them? [Yes]
2. If you are including theoretical results...
   (a) Did you state the full set of assumptions of all theoretical results? [N/A]
   (b) Did you include complete proofs of all theoretical results? [N/A]
3. If you ran experiments...
   (a) Did you include the code, data, and instructions needed to reproduce the main experimental results (either in the supplemental material or as a URL)? [No] We will release them upon acceptance.
   (b) Did you specify all the training details (e.g., data splits, hyperparameters, how they were chosen)? [Yes] For novel techniques, we report hyperparameters. For well-known methods, we use the default set of hyperparameters, as described in the references
   (c) Did you report error bars (e.g., with respect to the random seed after running experiments multiple times)? [No] We run large scale experiments (ImageNet-1k scale), and multiple runs are computationally unfeasible
   (d) Did you include the total amount of compute and the type of resources used (e.g., type of GPUs, internal cluster, or cloud provider)? [Yes] We include total amount of compute to generate the data. For well-known methods, we use standard hyperparameters, and the compute requiered is the same as the original methods.
4. If you are using existing assets (e.g., code, data, models) or curating/releasing new assets...
   (a) If your work uses existing assets, did you cite the creators? [Yes]
   (b) Did you mention the license of the assets? [Yes] We use code-snippets available online, and we will only release the references to the available websites.
   (c) Did you include any new assets either in the supplemental material or as a URL? [No]
   (d) Did you discuss whether and how consent was obtained from people whose data you're using/curating? [Yes] We use code-snippets available online, and we will only release the references to the available websites.

(e) Did you discuss whether the data you are using/curating contains personally identifiable information or offensive content? [Yes] We have manually checked the output of the scripts to ensure there is no offensive content.

5. If you used crowdsourcing or conducted research with human subjects...

(a) Did you include the full text of instructions given to participants and screenshots, if applicable? [N/A]

(b) Did you describe any potential participant risks, with links to Institutional Review Board (IRB) approvals, if applicable? [N/A]

(c) Did you include the estimated hourly wage paid to participants and the total amount spent on participant compensation? [N/A]